Electronic Supplementary Material (ESI) for Journal of Materials Chemistry A.

Atomic Co-N_4 and Co nanoparticles confined in COF@ZIF-67 derived core-shell carbon frameworks: Bifunctional non-precious metal catalysts toward ORR and HER

Minghao Liu,[ab] Qing Xu,[ac*] Qiyang Miao,[ad] Shuai Yang,[e] Ping Wu,ab Guojuan Liu,[ab] Jun He,[b] Chengbing Yu,[d*] and Gaofeng Zeng [ac*]

Experimental section

Materials: 2-Methylimidazole were purchased from Aladdin. 2,4,6-Trihydroxybenzene-1,3,5-tricarbaldehyde (TP) and 2,2'-bipyridine-5,5'-diamine (BPY) were purchased from Alfa. Cobalt nitrate hexahydrate, methanol (MeOH), tetrahydrofuran (THF), ethanol (EtOH) and potassium hydroxide (KOH) were from Sinopharm Chemical Reagent Co.,Ltd.

Catalyst preparation: In a typical synthesis of ZIF-67, 4 mmol 2-methylimidazole and 1 mmol cobalt nitrate hexahydrate were dissolved in 25 mL MeOH, respectively, which were mixed and stirred at 25 °C for 24 hours to obtain purple solid. The ZIF-67 solid was washed with MeOH and THF in sequence and then dried in vacuum. For the synthesis of COF@ZIF, 63 mg of TP in 50 mL THF and 83.7 mg of BPY in 50 mL THF were added into the mixture of ZIF-67 (500 mg) and THF (200 mL), which were then sonicated for 30 minutes and stirred at 25 °C for 24 hours to obtain ZIF-67-supported TP-BPY-COF (named as COF@ZIF). The collected COF@ZIF was washed with MeOH and THF in sequence and then dried in vacuum with the yield of 81% TP-BPY-COF. The as-prepared ZIF-67 and COF@ZIF were heated to 800 °C with a rate of 5 °C min^{-1} and kept for 1 hour in N_2 to yield ZIF_{800} and $COF@ZIF_{800}$, repectively.

Electrochemical performance tests: The $COF@ZIF_{800}$ catalyst (5 mg) was ultrasonic dispersed in a Nafion ethanol solution (0.25 wt.%, 500 μL) for 2 h to yield a homogeneous ink. The catalyst ink (12 μL) was pipetted onto a glassy carbon electrode (d = 5.00 mm, S = 0.196 cm^2) with a loading amount of 0.6 mg cm^{-2}. The commercial Pt/C catalyst (20 wt.% platinum on carbon black, BASF) was employed as a reference. The Pt/C catalyst ink and electrode were prepared by the same conditions to that of $COF@ZIF_{800}$. All the electrochemical measurements were conducted in a conventional three-electrode cell using the electrochemical workstation (Pine Research Instrumentation, USA) at room temperature. The Ag/AgCl (3 M KCl) and platinum wire were used as reference and counter electrodes, respectively. A rotating ring disk electrode (RRDE) with a Pt ring and a glassy carbon disk served as the substrate for the working electrode for evaluating the ORR activity and selectivity of various catalysts. The electrochemical experiments were conducted in O_2 saturated aqueous solution of KOH (0.1 M) for ORR and in N_2 saturated aqueous solution of KOH (1.0 M) for HER, respectively. The RRDE measurements were conducted at a rotation rate of 1600 rpm with a sweep rate of 10 mV s^{-1}. On the basis of ring and disk currents, the electron-transfer number (n) and four-electron selectivity of catalysts based on the H_2O_2 yield (H_2O_2 %) were calculated from the equations of $n = 4\ I_D/(I_R/N) + I_D$ and $H_2O_2\ \% = 200\ (I_R/N)/(I_R/N) + I_D$, where I_D and I_R are the disk and ring currents, respectively, and the ring collection efficiency N is 0.37. The Tafel slope was estimated by linear fitting of the polarization curves according to the Tafel equation ($h = b \times \log j + a$, where j is the current density and b is the Tafel slope). For the cyclic voltammetry (CV) tests, the potential range was circularly scanned between 0.15 and 1.1 V at a scan rate of 50 mV s^{-1} after purging O_2 gas for 30 min. To estimate the double layer capacitance, the electrolyte was deaerated by bubbling with nitrogen, and then the voltammogram was evaluated again in the deaerated electrolyte.

Characterization: Powder X-ray diffraction (PXRD) data were recorded on an Ultima IV diffractometer with Cu Kα radiation by depositing powder on glass substrate, from 2ϑ = 1.5° up to 60° with 0.02° increment. Nitrogen sorption isotherms were measured at 77 K with a TriStar II, Micromeritics. The Brunauer-Emmett-Teller (BET) method was utilized to calculate the specific surface areas. By using the non-local density functional theory (NLDFT) model, the pore volume was derived from the sorption curve. X-ray photoelectron spectroscopy (XPS) measurements were carried out on a Thermo Scientific K-Alpha XPS spectrometer using Al Kα X-ray source for radiation. Raman spectra were obtained from a Bruker SEN TERRA spectrometer employing a semiconductor laser (λ = 532 nm). High-resolution transmission electron microscope images were obtained by transmission electron microscopy (TEM, FEI Tecnai G2) installed with energy dispersive spectrometer (EDS, Oxford). The morphology was measured by a scanning electron microscope (SEM, Zeiss SUPRA 55 SAPPHIRE).

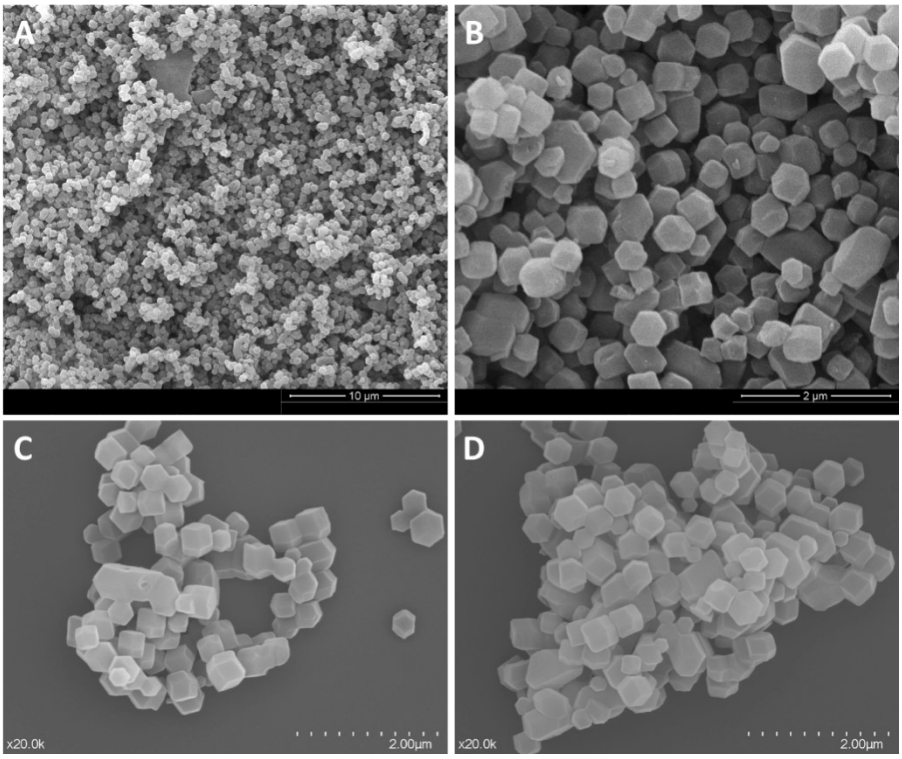

Figure S1. SEM images of ZIF-67.

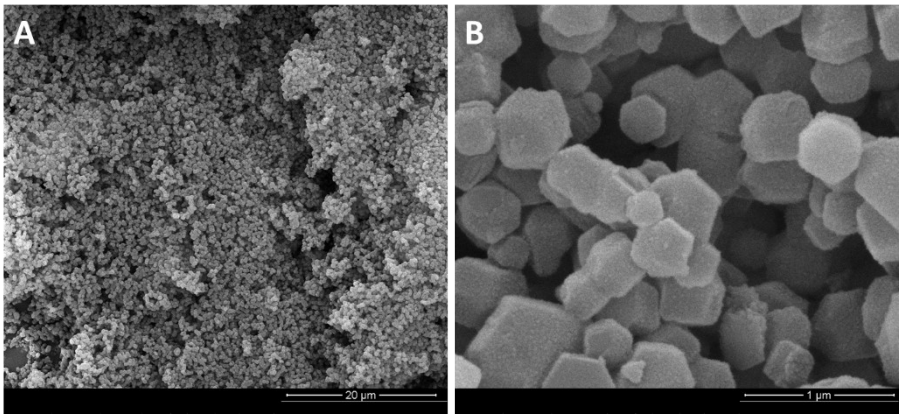

Figure S2. SEM images of COF@ZIF.

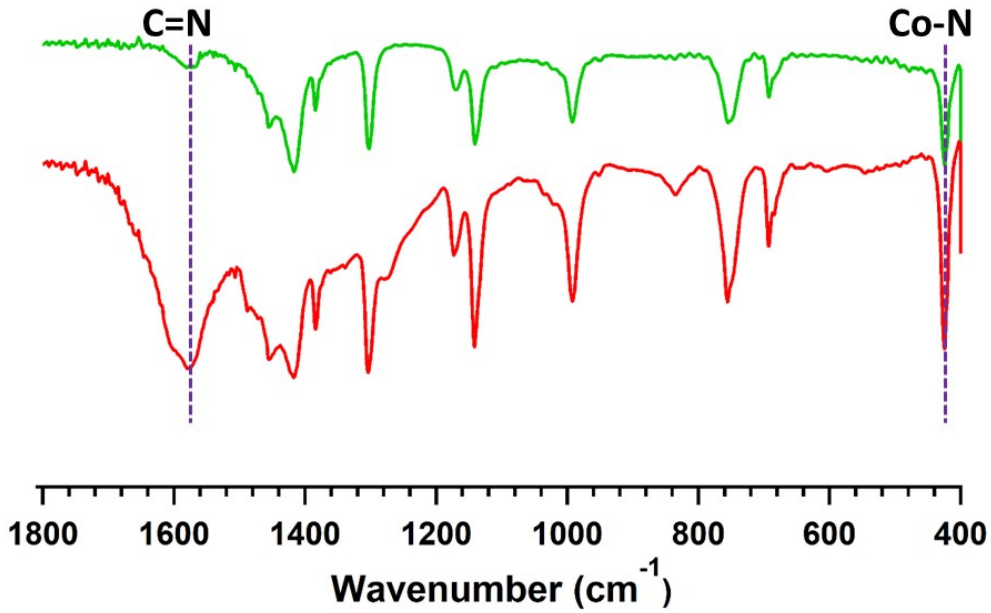

Figure S3. FT IR spectra of ZIF-67 (green) and COF@ZIF (red).

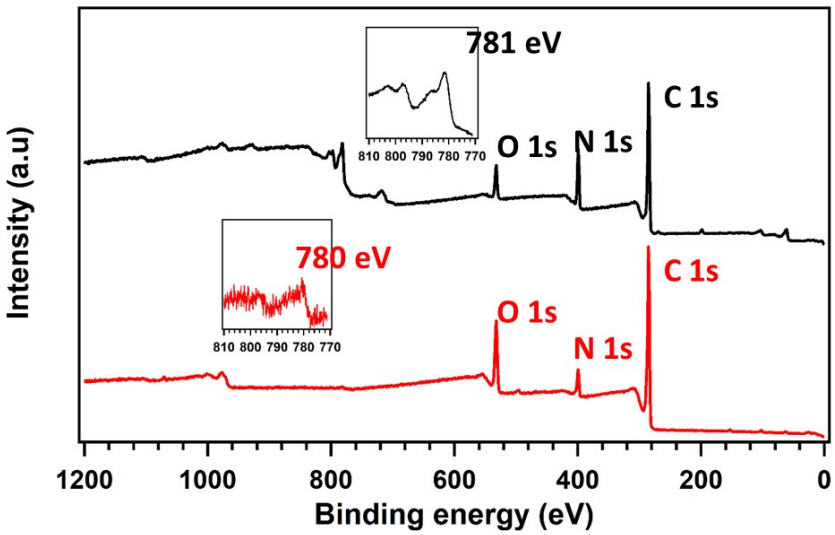

Figure S4. XPS spectra of ZIF-67 and COF@ZIF.

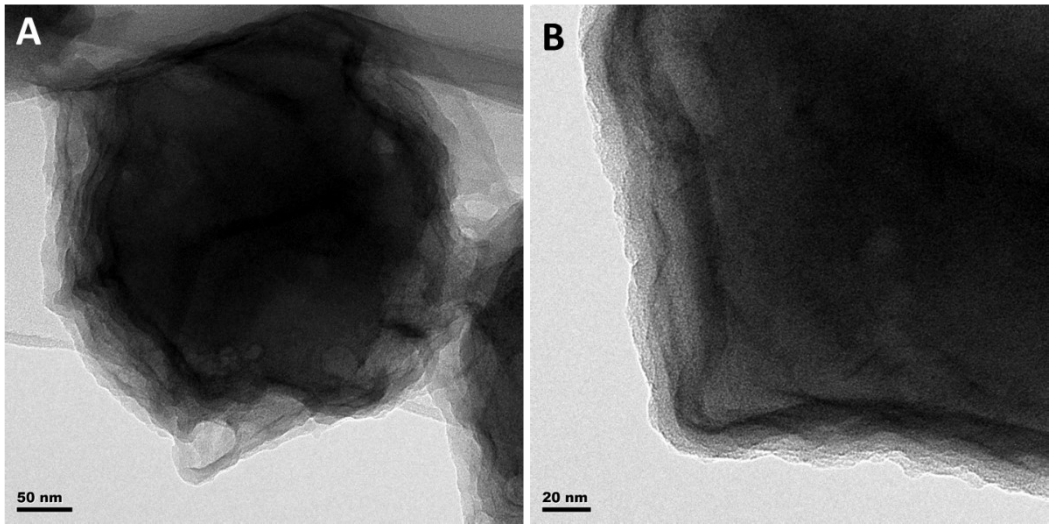

Figure S5. TEM images of COF@ZIF.

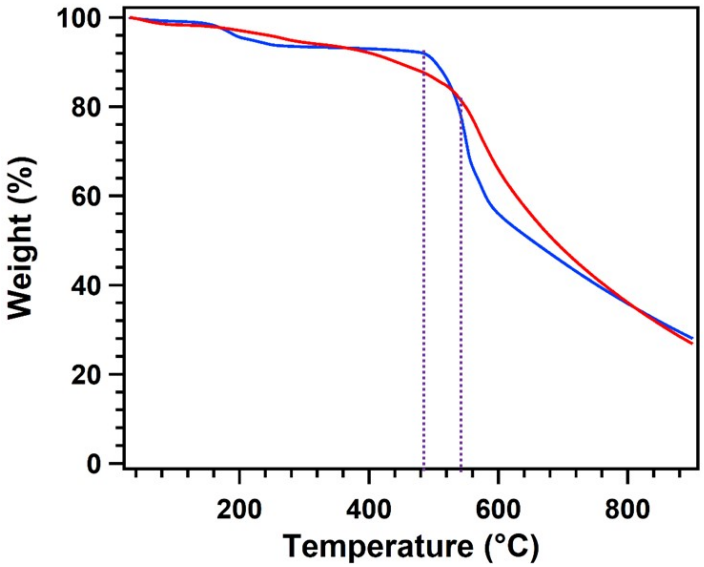

Figure S6. TGA profiles for ZIF-67 (blue curves) and COF@ZIF (red curve) from 25 to 900 °C under N_2.

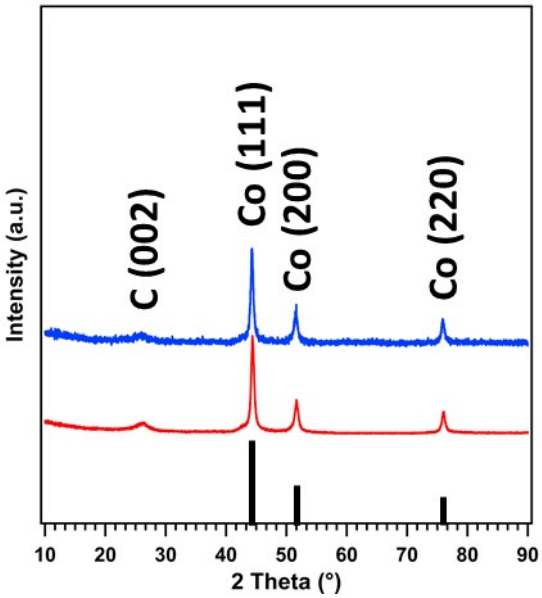

Figure S7. PXRD patterns of ZIF_{800} (blue), $COF@ZIF_{800}$ (red) and the standard of Co (black, PDF#15-0806).

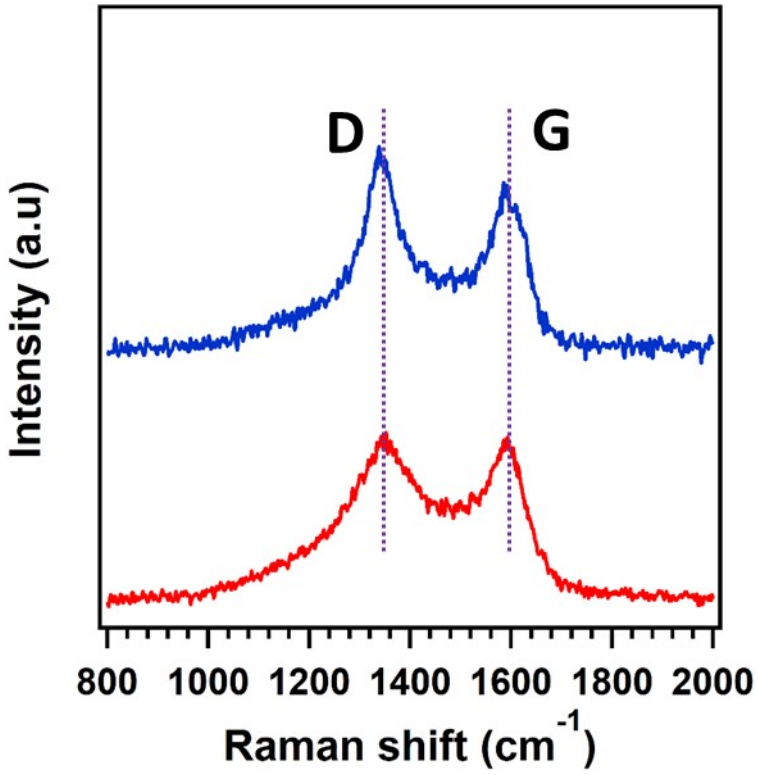

Figure S8. Raman spectra of ZIF_{800} (blue) and $COF@ZIF_{800}$ (red).

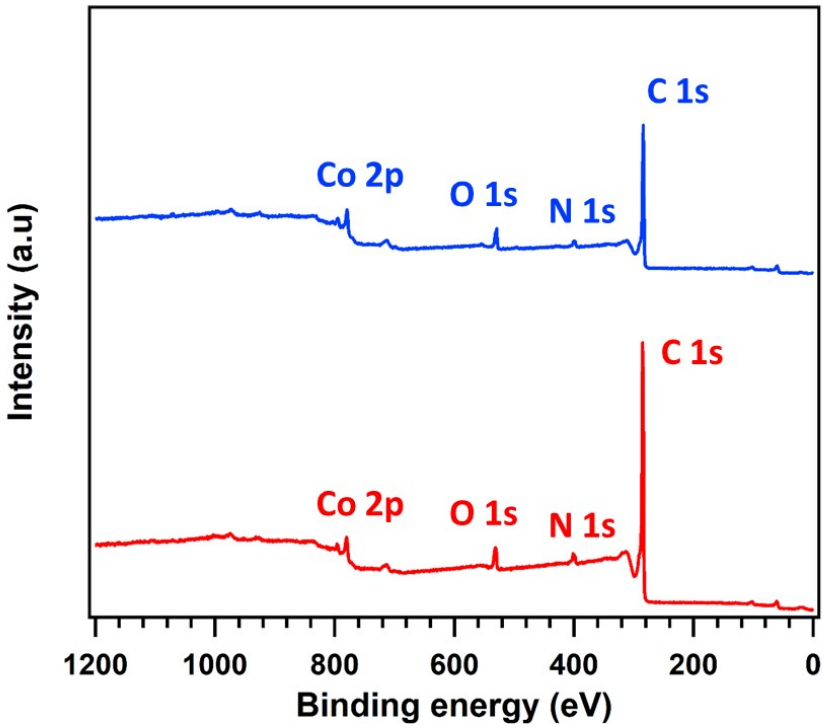

Figure S9. XPS spectra of ZIF_{800} (blue curve) and $COF@ZIF_{800}$ (red curve).

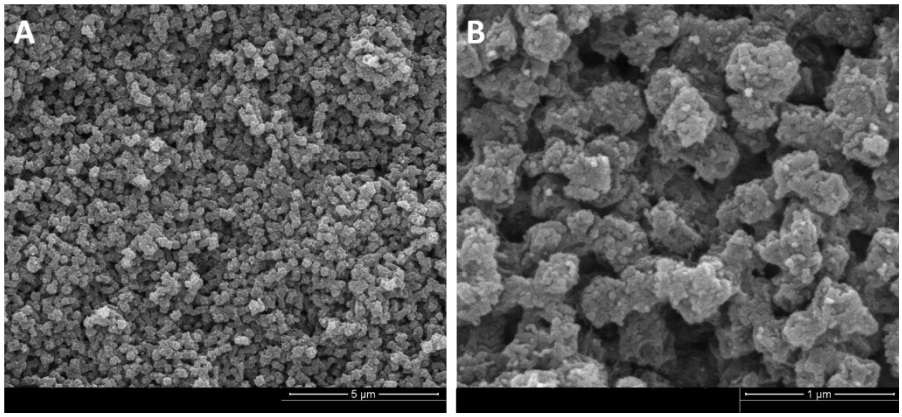

Figure S10. SEM images of ZIF_{800}.

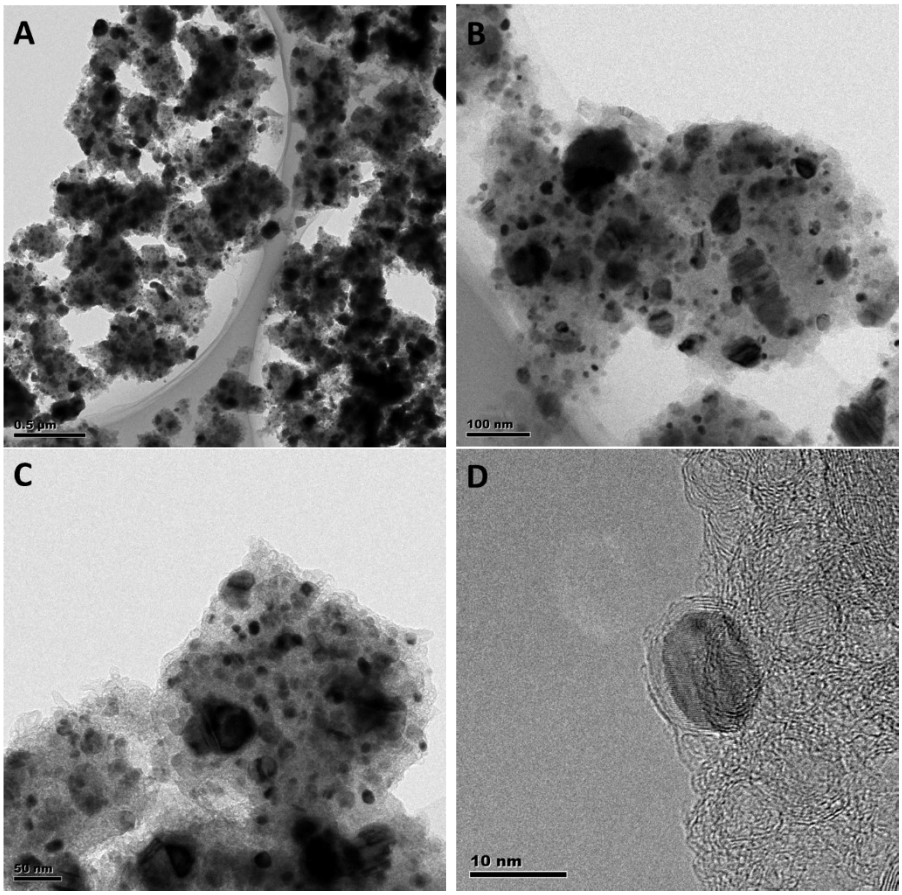

Figure S11. TEM images of ZIF_{800}.

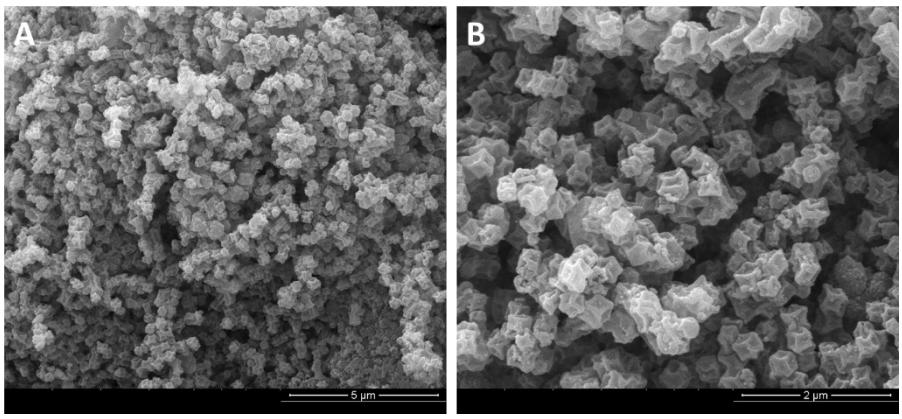

Figure S12. SEM images of COF@ZIF_{800}.

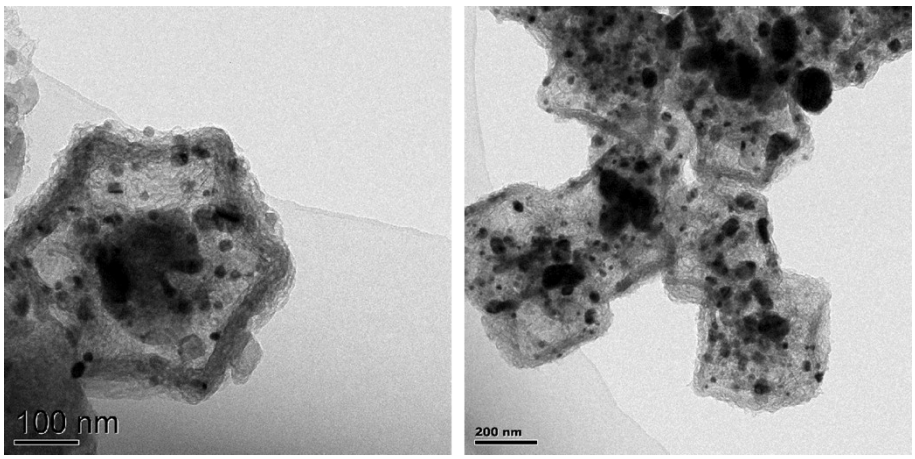

Figure S13. TEM images of COF@ZIF_{800}.

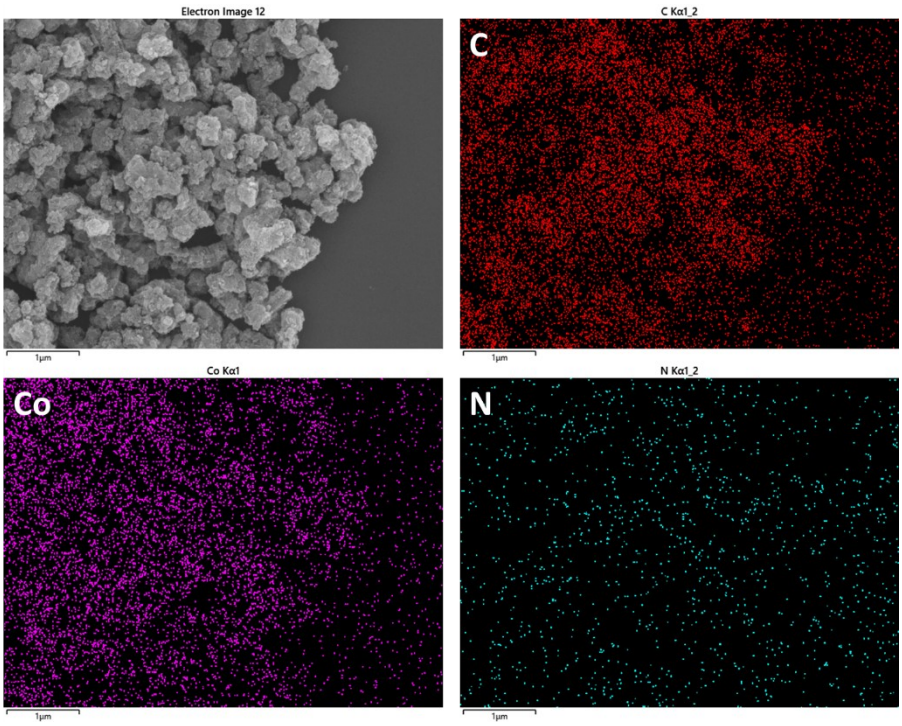

Figure S14. EDX mapping of ZIF_{800}.

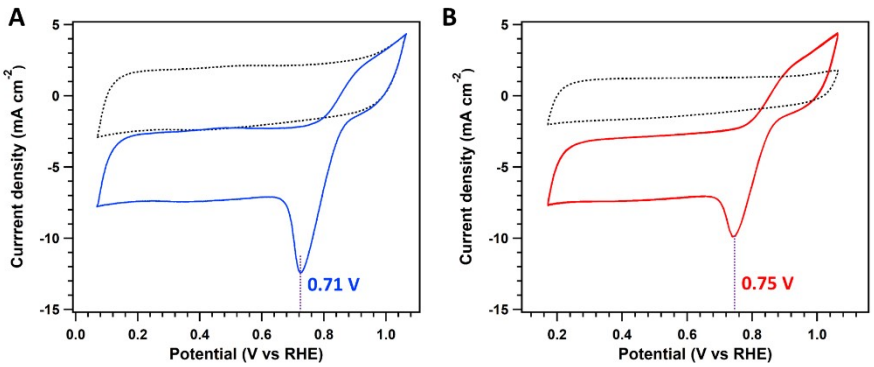

Figure S15. CV curves of ZIF_{800} (A) and $COF@ZIF_{800}$ (B).

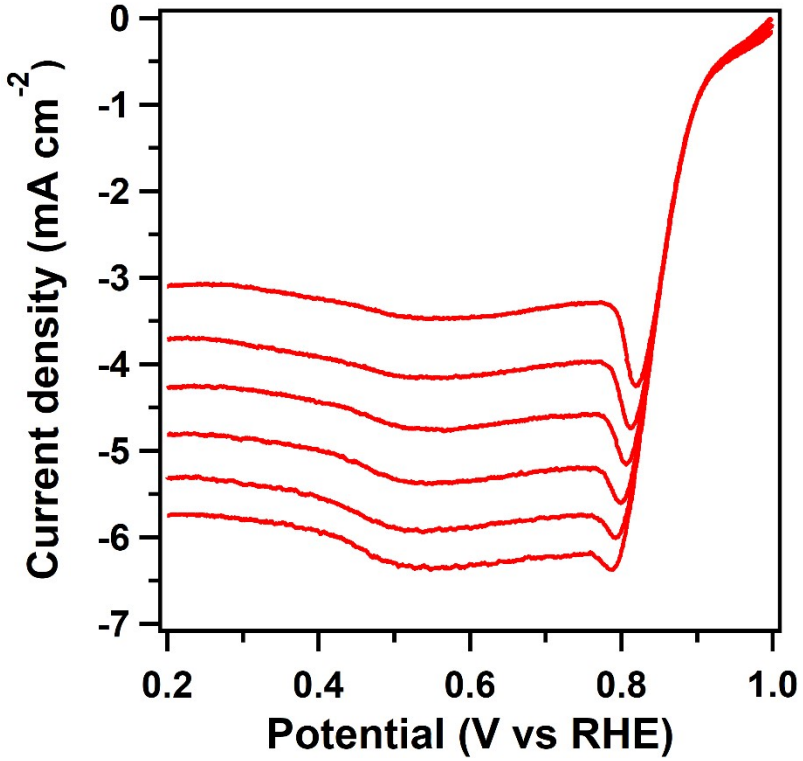

Figure S16. LSV curves for COF@ZIF_{800} at different scan rate.

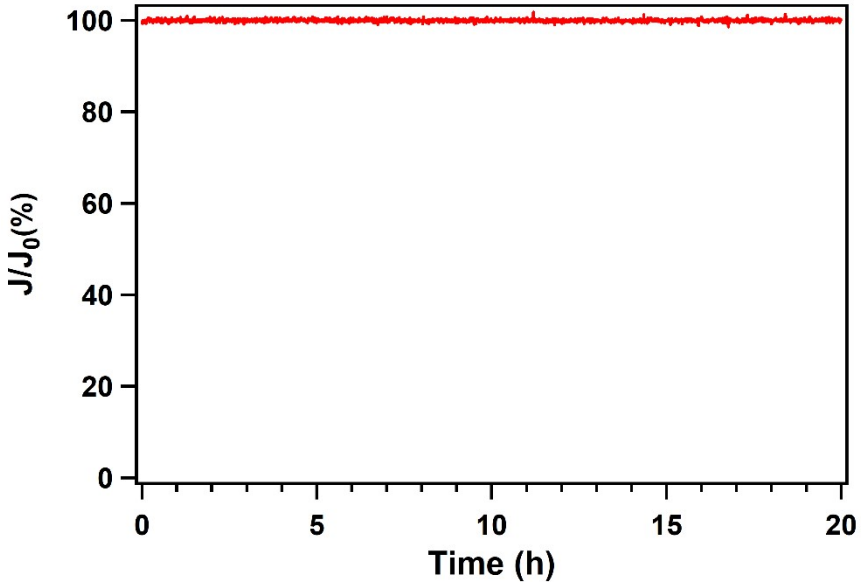

Figure S17. Long-term stability test of COF@ZIF_{800} at 0.6 V vs RHE for 20 h.

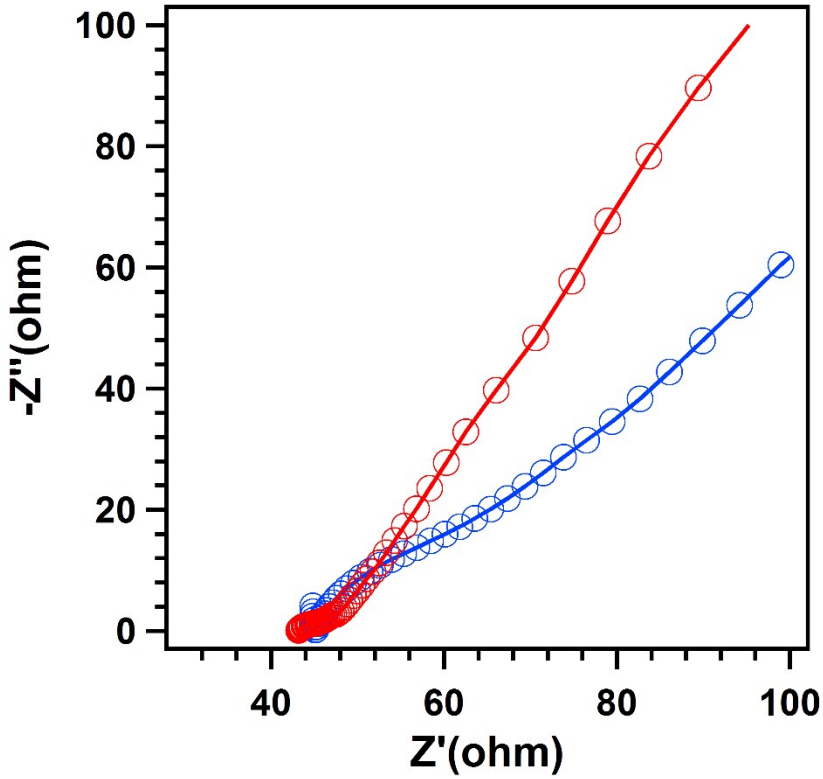

Figure S18. The EIS plots for COF@ZIF_{800} (red curves) and ZIF_{800} (black curves).

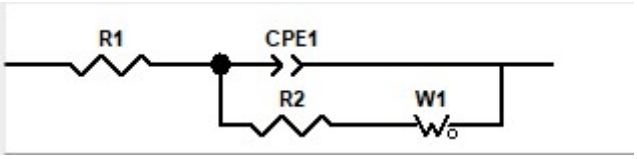

Figure S19. The diagram of EIS simulation circuit for COF@ZIF_{800} and ZIF_{800}.

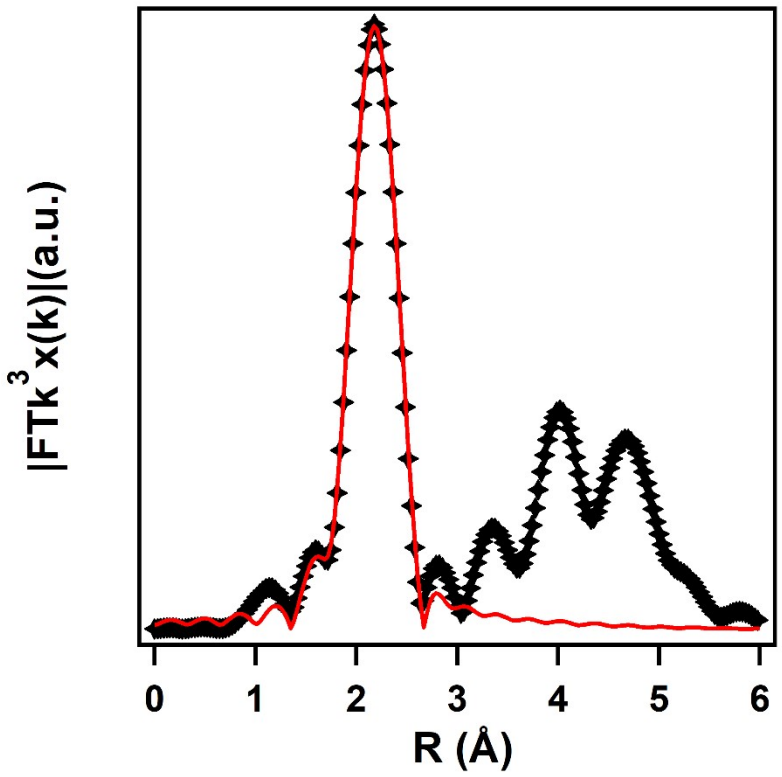

Figure S20. EXAFS fitting curve for Co in COF@ZIF$_{800}$.

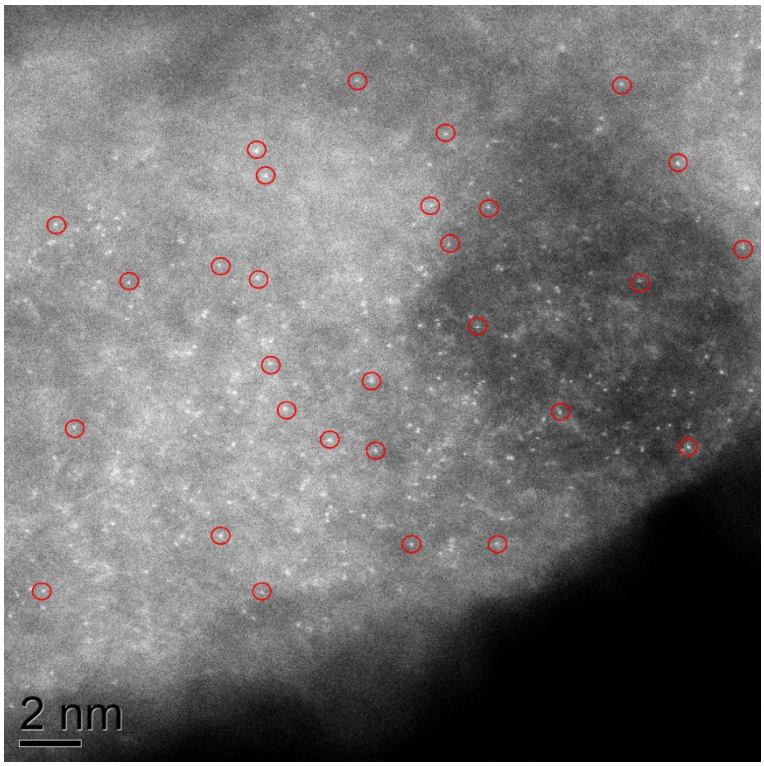

Figure S21. High-resolution HAADF-STEM images of COF@ZIF_{800}.

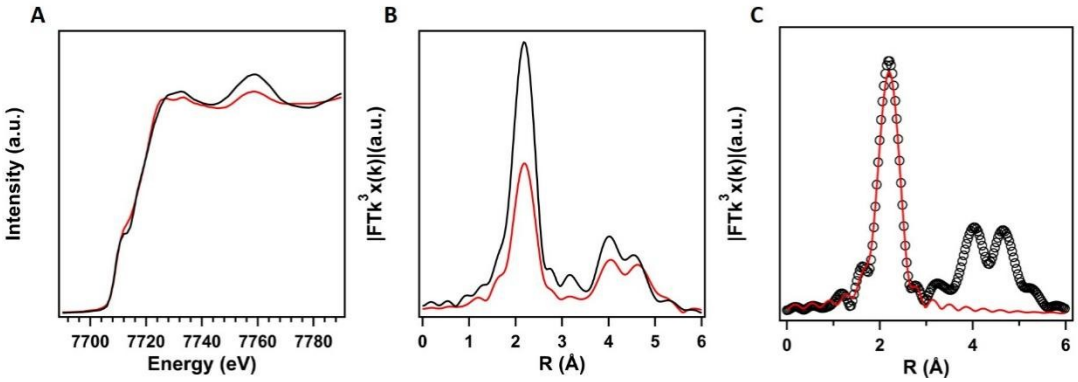

Figure S22. (A) X-ray absorption near-edge structure (XANES) spectra and (B) Fourier transformed k3-weightedχ(k)-function of the EXAFS spectra for ZIF_{800} (red) and Co foil (black) K-edge. (C) EXAFS fitting curve for Co in ZIF_{800}.

3. Tables

Table S1. Summary of electrocatalysts for ORR in 0.1 M KOH.

Catalysts	E_{onset} (V *vs.* RHE)	$E_{1/2}$ (V *vs.* RHE)	Tafel slope (mV dec^{-1})	Ref.
COF@ZIF$_{800}$	**0.99**	**0.85**	**44**	**This work**
Co-NC@600	0.94	0.83	66.5	1
Co_2P/CoN-NCNTs	0.96	0.85	49	2
CoTBrPP@bio-C	0.93	0.85	55	3
Co–NC@CC	0.94	0.81	76	4
Co–N_3C_1@GC	0.904	0.824	46	5
GC@COF-$NC_{0.08}$	0.923	0.841	78.4	6
W_2N/WC	0.93	0.81	58.13	7
FeP/Fe_2O_3@NPCA	0.95	0.838	88	8
Co/N-C(PA)	0.95	0.845	63	9
Co-SAs@NC	0.96	0.82	-	10
CAN-Pc(Fe/Co)	0.95	0.84	54	11
L-CCNTs-Co-800	0.90	0.84	54	12
CoNi@NCNT/NF	0.97	0.87	-	13
CoO_xNPs/BNG	0.95	0.805	57	14
Co-C_3N_4/CNT	0.90	0.85	68.4	15
cal-CoZIF-VXC72	0.92	0.84	45	16

Table S2. The kinetic current densities (J_{kin}) for COF@ZIF_{800} and Pt/C at different potentials in 0.1 M KOH.

Catalysts	J_{kin} at 0.9 V	J_{kin} at 0.85 V	J_{kin} at 0.8 V
COF@ZIF_{800}	0.96	3.01	10.56
Pt/C	0.91	2.56	7.18

Table S3. Summary of electrocatalysts for HER in 1 M KOH.

Catalysts	Overpotential @ J_{10} / mV	Tafel slope (mV dec^{-1})	Ref.
COF@ZIF$_{800}$	**159**	**92**	**This work**
CoTBrPP@bio-C	220	80	3
C-CoP	173	71.1	17
Co- Fe-B-P	173	96	18
$Cu_{0.3}Co_{2.7}P$/NC	220	122	19
FeP NPs@NPC	214	82	20
W_2N/WC	148.5	47.4	7
O-Co_2P	160	61.1	21
NiCoP/rGO	209	124	22
Co/CoP	253	78.8	23
CoP/CC	209	129	24
Co-Ni_3N	194	150	25
Hollow Co_3O_4 Microtube Arrays	190	90	26
$Cu_{0.3}Co_{2.7}$/NC-ZIFs	220	122	27
Co_9S_8@NOSC	320	105	28
$Co_{0.85}Se$/NiFe-LDH	320	160	29
$NiCo_2S_4$ NW/NF	210	50.9	30

Table S4. Co K-edge fitting parameters.

Sample	shell	N	R (Å)	ΔE_0 (eV)	$\sigma^2(10^{-3}Å^2)$	R-factor
Co-foil	Co-Co	12	2.49	8.4	6.3	0.001
COF@ZIF_{800}	Co-N	0.7	2.10	14.3	6.8	0.004
	Co-Co	8.4	2.49	8.7	6.4	
ZIF_{800}	Co-Co	8.5	2.50	8.5	7.8	0.006

N, coordination numbers; R, the internal atomic distance; σ^2, Debye-Waller factor; ΔE_0, the edge-energy shift.

Table S5. The relevant parameters about EIS simulation circuit for COF@ZIF_{800} and ZIF_{800}.

COF@ZIF_{800}	Element	Value	ZIF_{800}	Element	Value
	R1	42.28		R1	43.2
	CPE1-T	0.000271		CPE1-T	0.00041283
	CPE1-P	0.28783		CPE1-P	0.5657
	R2	42.18		R2	83.2
	W1-R	378.1		W1-R	2313
	W1-T	2.031		W1-T	0.24422
	W1-P	0.55611		W1-P	0.5968

References

1. S. Roy, S. Mari, M.K. Sai, S.C. Sarma, S. Sarkar, S.C. Peter, *Nanoscale*, 2020, **12**, 22718-22734.
2. Y. Guo, P. Yuan, J. Zhang, H. Xia, F. Cheng, M. Zhou, J. Li, Y. Qiao, S. Mu, Q. Xu, *Adv. Funct. Mater.*, 2018, **28**, 1805641.
3. X. Lv, Y. Chen, Y. Wu, H. Wang, X. Wang, C. Wei, Z. Xiao, G. Yang, J. Jiang, *J. Mater. Chem. A*, 2019, **7**, 27089-27098.
4. Y. Zhong, Y. Lu, Z. Pan, J. Yang, G. Du, J. Chen, Q. Zhang, H. Zhou, J. Wang, C. Wang, W. Li, *Adv. Funct. Mater.*, 2021, **31**, 2009853.
5. X. Hai, X. Zhao, N. Guo, C. Yao, C. Chen, W. Liu, Y. Du, H. Yan, J. Li, Z. Chen, X. Li, Z. Li, H. Xu, P. Lyu, J. Zhang, M. Lin, C. Su, S.J. Pennycook, C. Zhang, S. Xi, J. Lu, *ACS Catal*., 2020, **10**, 5862-5870.
6. S. Zhang, W. Xia, Q. Yang, Y. Valentino Kaneti, X. Xu, S.M. Alshehri, T. Ahamad, M.S.A. Hossain, J. Na, J. Tang, Y. Yamauchi, *Chem. Eng. J.*, 2020, **396**, 125154.
7. J. Diao, Y. Qiu, S. Liu, W. Wang, K. Chen, H. Li, W. Yuan, Y. Qu, X. Guo, *Adv. Mater.*, 2020, **32**, 1905679.
8. K. Wu, L. Zhang, Y. Yuan, L. Zhong, Z. Chen, X. Chi, H. Lu, Z. Chen, R. Zou, T. Li, C. Jiang, Y. Chen, X. Peng, J. Lu, *Adv. Mater.*, 2020, **32**, 2002292.
9. J. Du, G. Wu, K. Liang, J. Yang, Y. Zhang, Y. Lin, X. Zheng, Z.Q. Yu, Y. Wu, X. Hong, *Small*, 2021, **17**, 2007264.
10. X. Han, X. Ling, Y. Wang, T. Ma, C. Zhong, W. Hu, Y. Deng, *Angew. Chem. Int. Ed.*, 2019, **58**,5359-5364.
11. S. Yang, Y. Yu, M. Dou, Z. Zhang, L. Dai, F. Wang, *Angew. Chem. Int. Ed.*, 2019, **58**, 14724-14730.
12. Z. Liang, X. Fan, H. Lei, J. Qi, Y. Li, J. Gao, M. Huo, H. Yuan, W. Zhang, H. Lin, H. Zheng, R. Cao, *Angew. Chem. Int. Ed.*, 2018, **57**, 13187-13191.
13. W. Niu, S. Pakhira, K. Marcus, Z. Li, J.L. Mendoza-Cortes, Y. Yang, *Adv. Energy Mater.*, 2018, **8**, 1800480.
14. Y. Tong, P. Chen, T. Zhou, K. Xu, W. Chu, C. Wu, Y. Xie, *Angew. Chem. Int. Ed.*, 2017, **56**, 7121-7125.
15. Y. Zheng, Y. Jiao, Y. Zhu, Q. Cai, A. Vasileff, L.H. Li, Y. Han, Y. Chen, S.Z. Qiao, *J. Am. Chem. Soc.*, 2017, **139**, 3336-3339.
16. B. Ni, C. Ouyang, X. Xu, J. Zhuang, X. Wang, *Adv. Mater.*, 2017, **29**, 1701354.
17. W. Li, G. Cheng, M. Sun, Z. Wu, G. Liu, D. Su, B. Lan, S. Mai, L. Chen, L. Yu, *Nanoscale*, 2019, **11**, 17084-17092.
18. Z. Wu, D. Nie, M. Song, T. Jiao, G. Fu, X. Liu, *Nanoscale*, 2019, **11**, 7506-7512.
19. J. Song, C. Zhu, B.Z. Xu, S. Fu, M.H. Engelhard, R. Ye, D. Du, S.P. Beckman, Y. Lin, *Adv. Energy Mater.*, 2017, **7**, 1601555.
20. Z. Pu, I.S. Amiinu, C. Zhang, M. Wang, Z. Kou, S. Mu, *Nanoscale*, 2017, **9**, 3555-3560.
21. K. Xu, H. Ding, M. Zhang, M. Chen, Z. Hao, L. Zhang, C. Wu, Y. Xie, *Adv. Mater.*, 2017, **29**, 1606980.
22. J. Li, M. Yan, X. Zhou, Z.-Q. Huang, Z. Xia, C.R. Chang, Y. Ma, Y. Qu, *Adv. Funct. Mater.*, 2016, **26**, 6785-6796.

23. Z.H. Xue, H. Su, Q.Y. Yu, B. Zhang, H.H. Wang, X.-H. Li, J.S. Chen, *Adv. Energy Mater.*, 2017, **7**, 1602355.
24. J. Tian, Q. Liu, A.M. Asiri, X. Sun, *J. Am. Chem. Soc.*, 2014, **136**, 7587-7590.
25. C. Zhu, A.L. Wang, W. Xiao, D. Chao, X. Zhang, N.H. Tiep, S. Chen, J. Kang, X. Wang, J. Ding, J. Wang, H. Zhang, H.J. Fan, *Adv. Mater.*, 2018, **30**, e1705516.
26. Y.P. Zhu, T.Y. Ma, M. Jaroniec, S.Z. Qiao, *Angew. Chem., Int. Ed.*, 2017, **56**, 1324-1328.
27. J. Song, C. Zhu, B.Z. Xu, S. Fu, M.H. Engelhard, R. Ye, D. Du, S.P. Beckman, Y. Lin, *Adv. Energy Mater.*, 2017, **7**, 1601555.
28. S. Huang, Y. Meng, S. He, A. Goswami, Q. Wu, J. Li, S. Tong, T. Asefa, M. Wu, *Adv. Funct. Mater.*, 2017, **27**, 1606585.
29. Y. Hou, M.R. Lohe, J. Zhang, S. Liu, X. Zhuang, X. Feng, *Energy Environ. Sci.*, 2016, **9**, 478-483.
30. A. Sivanantham, P. Ganesan, S. Shanmugam, *Adv. Funct. Mater.*, 2016, **26**, 4661-4672.